cording to the temperature decrease support the aqueous phase theory of anesthesia. Also the fact that the presence of a fully active acidic hydrogen in anesthetizing molecule increases anesthetic potency[21] supports the aqueous phase theory.

Acknowledgement. This work was supported in part by the Korea Research Center for Theoretical Physics and Chemistry and the Korea Science and Engineering Foundation.

References

1. K.H. Meyer, *Trans. Faraday Soc.*, **33**, 1062(1937).
2. L.J. Mullins, *Chem. Rev.*, **54**, 289(1954).
3. (a) K.W. Miller, W.D.M. Paton, and E.B. Smith, *Nature*, **206**, 574(1965); (b) K.W. Miller, W.D.M. Paton, and E.B. Smith, *Anesthesiology*, **36**, 339(1972).
4. H. Eyring, J.W. Woodbury, J.S. D'Arrigo, *Anesthesiology*, **38**, 415(1973).
5. L. Pauling, *Science*, **134**, 15(1961).
6. S.L. Miller, *Proc. Nat. Acad. Sci.*, **47**, 1515(1961).
7. W.F. Clausen and M.F. Polglase, *J. Am. Chem. Soc.*, **74**, 4817(1952).
8. Y.K. Kang and M.S. Jhon, *Bull. Korean Chem. Soc.*, **2**, 8(1981).
9. J.H. van der Waals and J.C. Platteuw, *Advan. Chem. Phys.*, **2**, 1(1959).
10. G.A. Jeffrey and R.K. McMullan, *Progress in Inorganic Chemistry*, **8**, 43(1967).
11. The geometry of each anesthetizing molecule is taken from "Tables of interatomic distances and configuration in molecules and ions," ed. by L.E. Sutton, Special Publication No. 11, Burlington House, London, 1958.
12. D. Eisenberg and W. Kauzmann, "The Structure and Properties of Water," p. 4, Clarendon, Oxford, 1969.
13. R. Fletcher, "Fortran Subroutines for Minimization by Quasi-Newton Methods," A.E.R.E. Report R7125 (1972).
14. H.S. Frank and M.W. Evans, *J. Chem. Phys.*, **13**, 507(1945).
15. M.J. Moon and M.S. Jhon, *Bull. Chem. Soc. Jpn.*, **59**, 1215(1986).
16. R.D. Kaufman, *Anesthesiology*, **46**, 49(1977).
17. P.M. Winter, R.A. Smith, M. Smith, and E.I. Eger, *Anesthesiology*, **44**, 416(1976).
18. M.J. Lever, K.W. Miller, and W.D.M. Paton, *Nature*, **231**, 368(1971).
19. A. Cherkin and J.F. Catchpool, *Science*, **144**, 1460(1964).
20. (a) J.H. Hildebrand and R.C. Scott, "The Solubility of Nonelectrolytes," 3rd Ed., pp. 251-252, Reinhold, New York, 1950; (b) W. Gerrard, "Solubility of Gases and Liquids," pp. 231-234, Plenum, New York and London, 1976.
21. A. Spinks, *Chemistry and Industry*, **18**, 475(1977).

Geometries and Energies of S_N2 Transition States†

Ikchoon Lee,* Chan Kyung Kim, and Chang Hyun Song

Department of Chemistry, Inha University, Incheon 160. *Received August 1, 1986*

MNDO calculations were carried out to determine reactant complexes and transition states of the S_N2 reactions of $CH_3X + Y^- \rightarrow CH_3Y + X^-$ where X = F, Cl, CN and Y = CN, OH, F, Cl. The leaving group ability was found to vary inversely with the activation barrier, which in turn was mainly ascribable to the deformation energies accompanied with bond stretching of C-X bond and inversion of CH_3 group. The nucleophilicity was shown to be in the order $Cl^- > F^- > OH^- > CN^-$ but the effect on the activation barrier was relatively small compared with that of the leaving group. The bond breaking and bond formation indices and energy decomposition analysis showed that the TS for the reaction of CH_3Cl occurs in the early stage of the reaction coordinate relative to that of CH_3F. It has been shown that the potential energy surface (PES) diagrams approach can only accommodate thermodynamic effects but fails to correlate intrinsic kinetic effects on the TS structure.

Introduction

Experimental studies of gas-phase S_N2 reactions have been suggested that the potential energy profile will have the double-well form shown in Figure 1; two minima correspond to reactant (RC) and product complexes (PC), while the central barrier is the highest energy point on the minimum energy reaction path from RC to PC and can be identified as the classical S_N2 transition state (TS). The activation barrier is therefore given by the energy difference between the TS and RC, which can be estimated[1] from the intrinsic barriers for the identity reaction using Marcus equation.[2]

As S_N2 reaction, $Y^- + CH_3X \rightarrow YCH_3 + X^-$ proceeds via the concerted bond-breaking and bond-formation with a concomitant inversion of the reaction center carbon. Thus at the TS a number of changes in molecular geometry occur; the C-X bond stretches, the C-Y bond shortens and the H-C-H angles deform. These distortions in geometry are accompanied by changes in the total energy of the system. Mitchel *et al.*[3], has shown that in the identity S_N2 reaction, the distortion energies are dominated by the C-X stretching deformations which are linearly correlated with the intrinsic barriers.

In the work, we investigated the relationships between geometries and energies of the S_N2 (non-identity) reactions,

† Determination of Reactivity by MO Theory (Part 47).

(1), by carrying out MNDO calculations[4] on the reactant complex (RC) and TS involved in the reactions (1).

$$Y^- + CH_3X \rightarrow YCH_3 + X^- \quad (1)$$

where X=F, Cl, CN
Y=CN, OH, F, Cl

Calculations

The MNDO program[4] was used throughout in this work. For the reactions of CH_3F[10] and CH_3Cl[5], the results reported in the literature are used. For the reaction of CH_3CN the TS was obtained by using reaction coordinate method[6] and it was subsequently confirmed that the structure had only one negative eigenvalue in the Hessian metrix.[7]

In the ordinary force constant calculations, the C–X bond stretching force constant (f_R) appears as a mixture in the normal mode with the bond-bending component, so that in this work it was numerically calculated as a quotient of gradient changes to bond length changes with an increment of 0.01 Å.

Deformation energies were calculated only for the substrate part in the RC and TS.

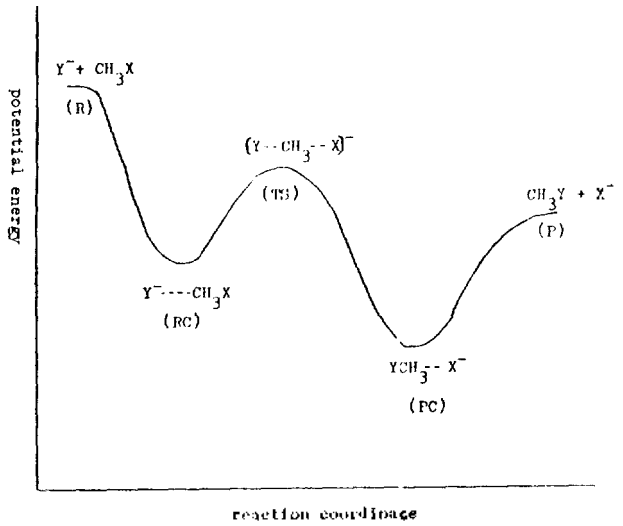

Figure 1. Potential energy profile for the gas-phase displacement reaction $Y^- + CH_3X \rightarrow YCH_3 + X^-$.

Results and Discussion

The S_N2 activation energy, ΔE^*, can be expressed as a sum of deformation energy, ΔE^*_{def}, accompanied with the structural distortion from the RC to TS, and the orbital interaction energy, ΔE^*_{int}, between the two distorted (to the TS geometries) reactants.[8]

$$\Delta E^* = \Delta E^*_{def} + \Delta E^*_{int} \quad (2)$$

The latter component ΔE^*_{int} is in general further decomposed into four parts, electrostatic, E_{es}, exchange repulsion, E_{ex}, polarization, E_{pl}, and change transfer, E_{ct}, terms.

$$\Delta E^*_{int} = E_{es} + E_{ex} + E_{pl} + E_{ct} \quad (3)$$

The deformation energy, ΔE^*_{def}, on the other hand, can be partitioned into the energy required to stretch C–X bond, the stretching deformation energy (ΔE_R), that required to bend H–C–H angles, the bending deformation energy (ΔE_θ) and that of the coupling term ($\Delta E_{R\theta}$) of the two effects.

$$\Delta E_{def} = \Delta E_R + \Delta E_\theta + \Delta E_{R\theta} \quad (4)$$

These component terms can be approximated using experimental dissociation energies and force constants:[3]

$$\Delta E_R^{app} = D\{1-\exp(-\beta\Delta R)\}^2;\ \beta = (f_R/2D) \quad (5a)$$

$$\Delta E_\theta^{app} = \tfrac{1}{2} f_\theta (\Delta\theta)^2 \quad (5b)$$

$$\Delta E_{R\theta} = f_{R\theta}(\Delta R)(\Delta\theta) \quad (5c)$$

where approximate component energies are denoted by the superscript "app". D is the experimental dissociation energy of C–X bond,[9] ΔR and $\Delta\theta$ are variations in bond length of C–X and in bond angle of H–C–H accompanied with the change from RC to TS and f_R, f_θ and $f_{R\theta}$ are the force constants for

Table 1. Calculated C–X bond force constant (f_R) and experimental dissociation energy (D) of CH_3X

X	f_R[a]	D[b,c]
F	0.740	108
Cl	0.321	84
CN	0.506	114

[a]In hartree bohr^{-2}. [b]In kcal/mol. [c]From reference 9.

Table 2. Activation Barrier, C–X and C–Y Bond Length Changes, and Approximate Stretching Deformation Energies (ΔE^{app}_R) for the Reactions $Y^- + CH_3X \rightarrow CH_3Y + X^-$[a]

X	F				Cl				CN			
Y / Property	CN	OH	F	Cl	CN	OH	F	Cl	CN	OH	F	Cl
ΔE^*	40.1	42.4	44.9	77.7	1.4	3.2	5.1	10.5	26.9	30.9	34.4	68.5
R_1[b]	1.358	1.361	1.360	1.357	1.833	1.839	1.837	1.830	1.458	1.459	1.458	1.458
R_2[c]	1.750	1.644	1.644	2.176	1.905	1.949	1.964	2.149	1.657	1.657	1.665	2.384
R_1'[d]	3.397	3.329	3.345	3.615	3.064	3.080	3.048	3.345	3.371	3.364	3.301	3.590
R_2'[e]	1.665	1.685	1.644	1.964	2.384	2.289	2.176	2.149	1.709	1.800	1.750	1.905
ΔR_R^{app}	47.4	32.0	32.1	86.9	1.6	3.5	4.5	19.6	14.6	14.5	15.5	87.0

[a]All energies in kcal/mol and all bond lengths in Å. [b]C–X bond length in CH_3X at the geometry of RC. [c]C–X bond length in CH_3X at the geometry of TS. [d]C–Y bond length at the geometry of RC. [e]C–Y bond length at the geometry of TS.

each deformation.

Calculated force constants for CH_3X are summarized in Table 1 together with the experimental dissociation energies. The force constants obtained in this work are somewhat overestimated relative to the values calculated by *ab initio* method;[3] however, the relative order of the values is seen to be consistent.

In Table 2, we have collected the activation barriers, the bond lengths of C–X and C–Y bonds in the RC and TS, and ΔE_R^{app} estimated using eq (5a) for each reaction.

The linear correlation coefficient between ΔE^* and ΔE_R in Table 2 was 0.921. The deformation energies in Table 2 are those approximated using force constants and experimental dissociation energies for CH_3X; we can however obtain the deformation energies directly from the optimized energy differences between two structures shown in Figure 2. Here the structure **1** and **2** have the optimized geometries of CH_3X in the RC and TS respectively, and the structures **3** and **4** correspond to the geometries of the RC with the C–X bond stretched to the length in the TS and geometries of the RC with the CH_3 deformed to that of the TS respectively. The total deformation energy, ΔE_{def} is given by the difference in energy

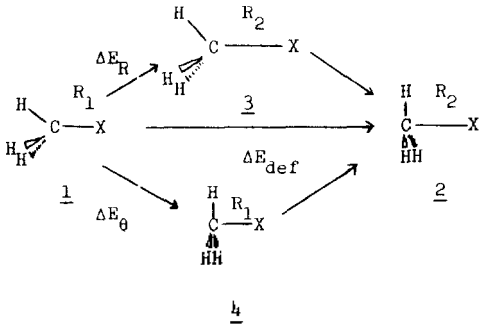

Figure 2. Geometrical representations used to calculate the deformation energy and its components. All quantities and structures are defined in the text.

between the structure **2** and **1**; the stretching deformation energy, ΔE_R and the bending deformation energy, ΔE_θ, are the energy differences between **3** and **1**, and between **4** and **1**, respectively. According to eq (2), interaction energies, ΔE^*_{int}, may be obtained by $\Delta E^*_{int} = \Delta E^* - \Delta E^*_{def}$. The results of these calculations are summzrized in Table 3. Good linearities[10] were obtained (r = 0.9) between deformation energies and ΔE^* for all three types shown in Table 3.

This is in contrast to the *ab initio* results[3] of little correlation between ΔE^* and ΔE_θ for identity reactions. The different behavior appears to stem from the fact that in the identity reaction TS is symmetric so that effects of nucleophile and leaving group almost cancel out in ΔE_θ values whereas in the non-identity reactions the effects on ΔE_θ become relatively large since the TS is not symmetric. The two contributions, ΔE_R and ΔE_θ to the total deformation energy are almost comparable so that bending of the H–C–H bonds also has large impact on the activation barriers in the non-identity S_N2 reactions studied in this work.

Reference to Table 3 also reveals that values of ΔE^*_{def} are positive while those of ΔE^*_{int} are negative, so that the former contributes to raise whereas the latter to lower the activation barrier. A striking feature to note, however, is that the magnitudes of the two values are nearly proportional; a greater degree of distortion requires a larger amount of energy on the one hand, but leads to a greater degree of orbital overlap causing stabilization of the system on the other hand. The two opposing effects on the energetics of ΔE^* have parallel changes but the effect of ΔE^*_{def} is grossly dominant so that overall changes in ΔE^* is determined by the values of ΔE^*_{def}, *i.e.*, $|\Delta E^*_{def}| \propto |\Delta E^*_{int}|$ but $|\Delta E^*_{def}| \gg |\Delta E^*_{int}|$.

In order to assess the "earliness" or "lateness" of the TS along the reaction coordinate, we defined the following two indices,

$$BB = 100\ \Delta R/R_1 \tag{6a}$$

$$BF = 100\ \Delta R'/R_1' \tag{6b}$$

Table 3. Calculated Deformation Energy, the Components, ΔE_R and ΔE_θ, of These Deformation Energy, and the Difference between Activation and Total Deformation Energy for the Reactions $Y^- + CH_3X \rightarrow CH_3Y + X^-$[a]

X	F				Cl				CN			
Y / Property	CN	OH	F	Cl	CN	OH	F	Cl	CN	OH	F	Cl
ΔE_R	62.3	40.6	40.6	131.7	2.8	5.5	6.7	25.3	25.5	17.4	18.6	133.8
ΔE_θ	55.6	44.1	43.8	92.4	2.6	4.8	6.2	24.5	36.1	27.5	28.1	86.5
ΔE_{def}	74.8	56.4	56.0	129.8	4.3	7.7	9.4	31.9	44.8	33.5	34.7	138.2
ΔE_{int}[b]	−34.7	−14.0	−11.1	−52.2	−2.8	−4.5	−4.3	−21.4	−17.9	−2.7	−0.4	−69.7

[a]All energies are in kcal/mol. [b]$\Delta E_{int} = \Delta E^* - \Delta E_{def}$.

Table 4. Bond Breaking (BB) and Bond Formation (BF) Indices for the S_N2 Reactions $Y^- + CH_3X \rightarrow CH_3Y + X^-$[a]

X	F				Cl				CN			
Y / Property	CN	OH	F	Cl	CN	OH	F	Cl	CN	OH	F	Cl
BB	28.9	20.8	20.9	60.4	4.0	6.0	6.9	17.4	13.6	13.5	14.1	63.5
BF	51.0	49.4	50.9	45.7	22.2	25.7	28.6	35.8	43.9	46.5	47.0	46.9

[a]All quantities are defined in eq (6).

where $\Delta R(=R_2 - R_1)$ and $\Delta R'(=R_2' - R_1')$ are the changes in the C–X and C–Y bond lengths from the RC to the TS as shown in Table 2 respectively. These indices represent the percentage of C–X lengthening and of C–Y shrinkage at the TS; large values of the indices will indicate large progress in the bond-breaking and -formation at the TS so that the TS is a "late" type, while small values will mean that the TS is at an "early" stage. The indices estimated are summarized in Table 4 for the reactions studied in this work.

Inspection of Tables 2 and 4 reveals a close correlation between the activation energies and the indices as the nucleophile and leaving groups are varied. Thus in the reactions of CH_3Cl, both indices are relatively small, predicting involvement of early type of TSs, which in turn have resulted in lower activation barriers[11] in accordance with the Hammond postulate.[12] In contrast, the S_N2 reactions of CH_3F are shown greater values of the indices and $\Delta E^{\ddagger}$ giving relatively "late" TSs. This is also in agreement with the poor leaving group ability of F^- compared to Cl^-. The S_N2 behaviors of CH_3CN are intermediate of those of the two compounds.

We have noted a proportionality between the magnitude of $\Delta E^{\ddagger}_{def}$ and that of $\Delta E^{\ddagger}_{int}$ above. Four components in eq (3) obtained from the energy decomposition analysis[13,14] are summarized in Table 5. For the reactions of CH_3Cl, the values of $\Delta E^{\ddagger}_{def}$ (Table 3) are shown to decrease in the order $Y=Cl^->F^->OH^->CN^-$, which is closely followed by the two *long range interaction* components of E_{es} and E_{pl}. This is another evidence in support of the early TS for the S_N2 reaction of CH_3Cl. Moreover inspection of energy components in Table 5 reveals that the *short range interaction* terms, E_{ex} and E_{ct}, are greater for the reactions of CH_3F than for the reactions of CH_3Cl in support of the relatively "late" TS involved in the S_N2 reactions of CH_3F. These results of energy decomposition analysis are in full accord with the conclusions reached from the indices BB and BF. The foregoing analysis of the trends in transition state geometries can be shown to be consistent with the predictions of potential energy surface (PES) diagrams.[15] In the PES diagram shown in Figure 3, if a change in X decreases the energies of the right hand side corners, as for X = Cl compared to X = F[16], the transition state o (e.g., for CH_3F) will shift to point c in accordance with the Hammond[12] (shifts to point a) and the anti-Hammond[17] (shifts to point b) vector sum rules. Irrespective of the relative stabilities of the two right side corners, CH_3Cl should have an earlier TS than CH_3F since the points a and c are all at the same distance on the reaction coordinate which is nearer towards reactants corner (R). Thus the TS for the S_N2 reaction of CH_3Cl will occur at relatively early stage on the reaction coordinate compared to that of CH_3F. This result is in contrast to the failure of the PES diagrams approach to correlate the TS structure with the intrinsic barriers for the identity S_N2 reactions.[3] It is therfore clear why we have two distinct behaviors of the PES diagrams approach in correlating the TS structure with the barrier heights of the S_N2 reactions: the approach is essentially of the thermodynamic nature. Thus any principle group, are equally important. A good leaving group X = Cl is characterized by an early TS relatively to a poor leaving group X = F. Finally the PES diagrams approach can only accommodate thermodynamic effects on the TS structure, but fails to correlate the intrinsic kinetic effects on the TS structure.

Table 5. Energy Decomposition Analysis of $\Delta E^{\ddagger}_{int}$ (hartree) for the Reaction of $CH_3X + Y^- \rightarrow CH_3Y + X^-$[a]

X	Cl				F
Y	Cl	F	OH	CN	F
E_{es}	-0.0654	-0.0318	-0.0292	-0.0287	-0.0720
E_{ex}	0.1115	0.0241	0.0221	0.0415	0.1894
E_{pl}	-0.0107	-0.0103	-0.0087	-0.0059	-0.0176
E_{ct}	-0.0589	-0.0822	-0.0412	-0.0187	-0.1753

[a]Morokuma STO-3G program[13] was used. In this calculation, two reactants with the TS geometries were brought to the bond distance at the TS and the energy change of interaction was obtained.

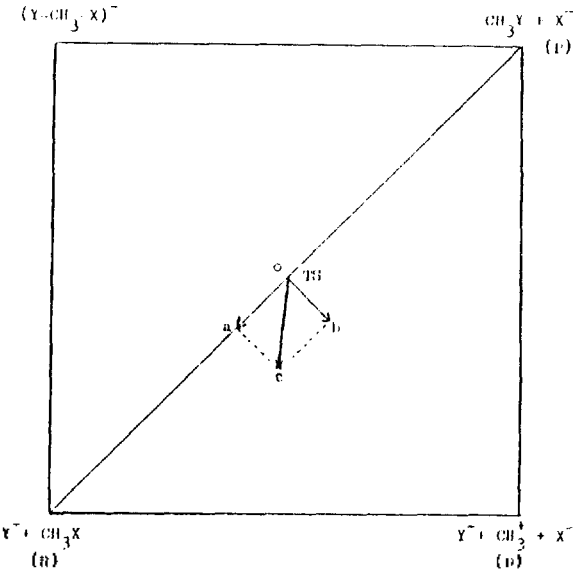

Figure 3. Potential energy surface diagram for the S_N2 reaction of $Y^- + CH_3X \rightarrow CH_3Y + X^-$. R, P and D denote reactants, products and dissociated corners, respectively.

Acknowledgements. This work is supported by the Ministry of Education and the Korea Science and Engineering Foundation.

References

1. (a) S. Wolfe, D.J. Mitchell, and H.B. Schlegel, *J. Am. Chem. Soc.*, **103**, 7692 (1981) (b) I. Lee, B-S Lee, and C.H. Song, *Bull. Korean Chem. Soc.*, **6**, 191 (1985).
2. (a) R.A. Marcus, *J. Phys. Chem.*, **72**, 891 (1968) (b) I. Lee and H. K. Kang, *Prog. Chem. Chem. Indus.*, **24**, 457 (1984).
3. D.J. Mitchell, H.B. Schlegel, S.S. Shaik, and S. Wolfe, *Can. J. Chem.*, **63**, 1642 (1985).
4. M.J.S. Dewar and W. Thiel, *J. Am. Chem. Soc.*, **99**, 4899, 4907, 5231 (1977).
5. F. Carrian and M.J.S. Dewar, *J. Am. Chem. Soc.*, **106**, 3531 (1984).
6. (a) M.J.S. Dewar, G.P. Ford, M.L. McKee, H.S. Rzepa, and L.E. Wade, *J. Am. Chem. Soc.*, **93**, 4290 (1971). (b) S. Bell and J.S. Crighton, *J. Chem. Phys.*, **80**, 2464 (1984).
7. J.W. McIver, Jr and A. Komornicki, *J. Am. Chem. Soc.*, **94**, 2629 (1972).
8. K. Kitaura and K. Morokuma, *Int. J. Quan. Chem.*, **10**,

325 (1976).
9. F.A. Carey and R.J. Sundberg, "Advanced Organic Chemistry," Part A, 2nd ed., New York, Plenum Press, 1984, p. 11
10. The correlation coefficients between $\Delta E^{\ddagger}$ and ΔE_R, ΔE_P, and ΔE_{av} are 0.905, 0.967, and 0.946, respectively.
11. In the CH_3Cl series, the RC is higher in energy than the PC. Therefore the TS resembles the RC in energy and structure.
12. G.S. Hammond, *J. Am. Chem. Soc.*, **77**, 334 (1955).
13. (a) W.A. Lathan and K. Morokuma, *J. Am. Chem. Soc.*, **97**, 3615 (1975) (b) H. Umeyama and K. Morokuma, *J. Am. Chem. Soc.*, **99**, 1316 (1977).
14. I. Lee and C.H. Song, *Bull. Korean Chem. Soc.*, **7**, 186 (1986).
15. J.M. Haaish, S.G. Shafer, J.R. Moffatt, and A.R. Becker, *J. Am. Chem. Soc.*, **101**, 3296 (1979).
16. Since the dissociation energy of the C-Cl bond is lower by 24 kcal/mol than that of C-F bond (Table 1), the P and D corners for X = Cl will be lower (or stabilized) by the same amount than for X = F.
17. E.R. Thorton, *J. Am. Chem. Soc.*, **89**, 2915 (1967).
18. R.P. Bell, *Proc. R. Soc. London, Ser. A*, **154**, 414 (1936).
19. M.G. Evans and M. Polanyi, *J. Chem. Soc., Faraday Trans.*, **32**, 1340 (1936).

MNDO Studies on Intramolecular Proton Transfer Equilibria of Acetamide and Methyl Carbamate[1]

Ikchoon Lee,* Chang Kon Kim, and Heon Su Seo

Department of Chemistry, Inha University, Inchon 160. *Received July 29, 1986*

Intramolecular proton transfer equilibria of acetamide and methyl carbamate have been studied theoretically by MNDO MO method. For both substrates, carbonyl-O protonated tautomer was found to be the most stable form, the next most stable one being N-protonated form. Gas phase proton transfers take place by the 1,3-proton rearrangement process and in all cases have prohibitively high activation barriers. When however one solvate water molecule participates in the process, the barriers are lowered substantially and the process proceeds in an intermolecular manner through the intermediacy of the water molecule via a triple-well type potential energy surface; three wells correspond to reactant(RC), intermediate(IC) and product complexs(PC) of proton donor-acceptor pairs whereas two transition states(TS) have proton-bridge structure. General scheme of the process can be represented for a substrate with two basic centers(heteroatoms) of A and B as,

$$\underset{}{\overset{+}{ABH}} + H_2O \rightarrow \underset{RC}{\overset{+}{ABH\cdots OH_2}} \rightarrow \underset{TS\ 1}{\overset{+}{AB\cdots H\cdots OH_2}} \rightarrow \underset{IC}{\overset{+}{AB\cdots HOH_2}}$$

$$\underset{}{\overset{+}{BAH}} + H_2O \leftarrow \underset{PC}{\overset{+}{BAH\cdots OH_2}} \leftarrow \underset{TS\ 2}{\overset{+}{BA\cdots H\cdots OH_2}}$$

Involvement of a second solvate water had negligible effect on the relative stabilities of the tautomers but lowered barrier heights by 5~6 Kcal/mol. It was calculated that the abundance of the methoxy-O protonated tautomer of the methyl carbamate will be negligible, since the tautomer is unfavorable thermodynamically as well as kinetically. Fully optimized stationary points are reported.

Introduction

Intermolecular proton transfers[2] and proton exchanges[3] in amides and related compounds have been of considerable interest because of their widespread importance in a large number of chemical and biological processes. On the other hand, information concerning intramolecular proton transfers between functional groups within a substrate forming various protonated tautomers is essential in elucidating mechanism of the hydroiysis of amides and carbamates in acid solution.[4]

The mechanims of A2 reaction of amides and carbamates[4] in strong acidic media should depend on which protonated form(carbonyl O-, N-, or alkoxy O-protonated form) is involved in the rate-determining attack of water on the protonated substrate. Currently the addition of water to the N-protonated tautomer(II) in the rate-determining step is favored for the mechanism of hydrolysis of protonated carbamates.[4] Hence it is believed to involve two steps, the

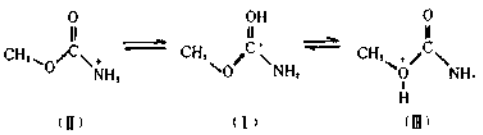

(II) (I) (III) (1)

pre-equilibrium between the dominant carbonyl O-protonated tautomer(I) and the minor N-protonated form(II), and the rate-determining nucleophilic attack of water on (II).

In this work we investigated the proton transfer equilibria